Brain, Behavior, and Immunity 134 (2026) 106484

Contents lists available at ScienceDirect

Brain Behavior and Immunity

journal homepage: www.elsevier.com/locate/ybrbi

Bright light therapy influences glymphatic system function in individuals with subthreshold depression: a randomized clinical trial

Pan Chen [a,b,1], Guanmao Chen [a,b,1], Zixuan Guo [a,b,1], Ruoyi Chen [a,b], Xinyue Tang [a,b], Zibin Yang [a,b], Wenhao Ma [c,d], Chao Chen [a,b], Shilin Sun [a,b], Yuan Zhang [c,d], Hui Zhong [e], Shu Zhang [c,d], Zhangzhang Qi [a,b], Wenjie Fang [c,d], Lijun Jiang [c,d], Zhinan Yin [e], Li Huang [a,b], Junxian Ma [f], Qian Tao [c,d,*], Ying Wang [a,b,**]

[a] Medical Imaging Center, First Affiliated Hospital of Jinan University, Guangzhou 510630, China
[b] Institute of Molecular and Functional Imaging, Jinan University, Guangzhou 510630, China
[c] Department of Public Health and Preventive Medicine, School of Basic Medicine, Jinan University, Guangzhou 510632, China
[d] Division of Medical Psychology and Behavior Science, School of Basic Medicine, Jinan University, Guangzhou 510632, China
[e] Biomedical Translational Research Institute, Jinan University, Guangzhou 510630, China
[f] Optical Brain Modulation Group, Tianfu Xinglong Lake Laboratory, Sichuan Province, China

ARTICLE INFO

Keywords:
Light therapy
Glymphatic system
Diffusion tensor image analysis along the perivascular space
Resting-state functional MRI
Inflammation
Subthreshold depression

ABSTRACT

Glymphatic system dysfunction is a potential early biomarker for neuropsychiatric disorders. This study aimed to evaluate the effects of bright light therapy (BLT) on the glymphatic system in individuals with subthreshold depression (StD) and its connections to brain activity, inflammatory cytokines, and depressive symptoms. A randomized placebo-controlled trial assigned adults with StD (N = 110) to 8 weeks of morning BLT (5000 lx, 30 min/day; n = 57) or placebo (inactive device; n = 53). Depression severity (primary outcome, including anhedonia), glymphatic markers (diffusion tensor image analysis along the perivascular space [DTI-ALPS] index, free water [FW], perivascular space volume), regional homogeneity (ReHo; functional MRI), and serum pro-inflammatory cytokines were assessed at baseline and post-treatment. Compared to placebo, BLT significantly relieved depressive symptoms, increased DTI-ALPS index, and decreased FW from baseline to post-treatment. BLT also increased ReHo in the left superior frontal gyrus (SFG) and decreased levels of interleukin-9 and tumor necrosis factor-β. Changes in the DTI-ALPS index correlated with ameliorated depressive symptoms, increased ReHo in the SFG, and decreased inflammatory cytokine levels. Additionally, the pairwise interaction effects between glymphatic markers, ReHo values, and serum levels of pro-inflammatory cytokines were independent predictors of improvements in depressive symptoms, particularly anhedonia. BLT may influence glymphatic function in StD, with enhanced glymphatic function correlated with reduced inflammation, enhanced prefrontal cortex activity, and symptom amelioration.

1. Introduction

Subthreshold depression (StD), often referred to as subclinical, mild, or subsyndromal depression, is considered a precursor to major depressive disorder (Cuijpers et al., 2021) and is associated with decreased health-related quality of life and increased disease burden and suicide rates (Cuijpers et al., 2014). Consequently, timely and effective intervention for StD is essential. Bright light therapy (BLT) is a safe, effective, and feasible treatment for both seasonal (Terman and Terman, 2005) and nonseasonal depression (de Almeida et al., 2025) (including StD (Jiang et al., 2020; Jiang et al., 2021)). Existing evidence establishes light therapy as a rapid-acting antidepressant modality with superior early efficacy compared to pharmacotherapy (Geoffroy et al., 2019; Lam et al., 2016; Rohan et al., 2015).

The glymphatic (glial–lymphatic) system is a fluid-transport system that accesses all regions of the brain (Iliff et al., 2012). The glymphatic

* Corresponding author at: Department of Public Health and Preventive Medicine, School of Basic Medicine, Jinan University, Guangzhou 510632, China.
** Corresponding author at: Medical Imaging Center, First Affiliated Hospital of Jinan University, Guangzhou 510630, China.
E-mail addresses: taoqian16@jnu.edu.cn (Q. Tao), johneil@vip.sina.com (Y. Wang).
[1] Pan Chen, Guanmao Chen and Zixuan Guo contributed equally to this work.

https://doi.org/10.1016/j.bbi.2026.106484
Received 28 September 2025; Received in revised form 13 January 2026; Accepted 8 February 2026
Available online 9 February 2026

system is an astrocyte-dependent waste clearance pathway that drives the movement of cerebrospinal fluid (CSF) via perivascular spaces. This process, which depends on aquaporin-4 (AQP4) expression on astrocytic endfeet, serves to deliver nutrients and neuroactive substances and remove metabolic waste, thereby maintaining brain homeostasis (Iliff et al., 2012; Xiong et al., 2024). Owing to its significant physiological functions, the glymphatic system is believed to be related to the occurrence and development of a variety of diseases, including neurovascular (Rasmussen et al., 2018), neuroinflammatory (Zou et al., 2024), and neurodegenerative diseases (Nedergaard and Goldman, 2020; Rasmussen et al., 2018), as well as mood disorders (Zhang et al., 2022a). For example, several studies revealed impaired glymphatic system function, characterized by significant neuroinflammation, reduced arterial pulsation and compliance, altered expression of astrocytic AQP4, and decreased clearance of exogenous β-amyloid (Aβ), in animal models of depression (Liu et al., 2020; Xia et al., 2017; Yao et al., 2023). Furthermore, the antidepressant fluoxetine improved glymphatic pathway circulation via the regulation of AQP4 recovery (Xia et al., 2017). The results of preclinical studies suggest that glymphatic function can be influenced by pharmacological (Lohela et al., 2022; Sun et al., 2018) and nonpharmacological interventions (Salehpour et al., 2022; von Holstein-Rathlou et al., 2018; Xie et al., 2013). Light stimulation enhances glymphatic function and improves cognitive performance in mouse models of neurodegenerative diseases (Murdock et al., 2024; Sun et al., 2024a), which might be attributable to increased neuronal activity. Recent studies have shown that visual light can accelerate glymphatic clearance in the visual cortex of mice (van Veluw et al., 2020) and increase CSF flow in the human brain (Williams et al., 2023a). BLT may regulate key components of the perivascular drainage pathway, including vascular pulsation, AQP4 polarization, and slow-wave activity (Bissig et al., 2020; Sun et al., 2024a; Wu et al., 2025; Zhao et al., 2025), which constitute the most fundamental structure and intervention target of the glymphatic system. However, the potential impact of BLT on the glymphatic system in participants with StD has not been studied.

The glymphatic system has been investigated via a variety of methodologies, including ex vivo fluorescence microscopy and in vivo two-photon imaging in animal models, as well as intrathecal contrast medium-enhanced magnetic resonance imaging (MRI) and dynamic positron emission tomography (PET) in human subjects (Bohr et al., 2022). Recently, novel MRI-based approaches enabling non-invasive in vivo assessment of human glymphatic function have emerged (Li et al., 2024; S. Lin et al., 2024). These include volumetric measurement of perivascular spaces (PVS) to assess their drainage capacity, quantification of free water (FW) as an extracellular water fraction reflecting interstitial fluid dynamics, and diffusion tensor image analysis along the perivascular space (DTI-ALPS) to estimate glymphatic activity via the DTI-ALPS index (Taoka et al., 2017). DTI-ALPS provides a real-time and noninvasive method to evaluate the human glymphatic system without the need for intravenous or intrathecal injections of contrast agent. Moreover, the results of this method are significantly associated with those of the intrathecal method of glymphatic measurement and exhibit good reliability and reproducibility (Carotenuto et al., 2022; Zhang et al., 2021). Several studies have identified altered DTI-ALPS indices in individuals with neurodegenerative (Kamagata et al., 2022; Shen et al., 2022; Taoka et al., 2017) and psychiatric diseases (Bae et al., 2023; Siow et al., 2022; Tu et al., 2024) (including mood disorders (Ueda et al., 2024)). Thus, some researchers have proposed that glymphatic dysfunction is likely a common feature of central nervous system diseases that may emerge in early disease stages (Liu et al., 2024; Nedergaard and Goldman, 2020).

In this randomized, placebo-controlled trial, we examined the effects of an 8-week BLT intervention on glymphatic function, as measured by the DTI-ALPS index, FW and perivascular space (PVS) volume, in individuals with StD. Furthermore, we explored the relationships between BLT-induced alterations in glymphatic function and changes in brain functional activity (regional homogeneity [ReHo]), pro-inflammatory cytokine levels, and depressive symptoms. We hypothesize that, compared to placebo, BLT would lead to changes compatible with enhanced glymphatic function, specifically a relative increase in the DTI-ALPS index and decreases in PVS volume and FW. We planned to explore whether the observed changes in glymphatic metrics were associated with concurrent changes in spontaneous brain activity, levels of specific pro-inflammatory cytokines, and depressive symptom severity. This study provides the first direct test in humans of whether glymphatic function is a modifiable target of BLT and a key mechanistic pathway linking circadian therapy to neuroimmune and clinical outcomes in early depression.

2. Methods

2.1. Study design

A randomized controlled trial (RCT) was conducted to evaluate the efficacy of BLT for treating StD. The BLT group was treated for 8 weeks, and the placebo group was treated with an inactive device for 8 weeks. The study employed a double-blind design using a simple randomization procedure. Using a computer-generated sequence created before the trial, participants were assigned in a 1:1 ratio to either the BLT or placebo group in strict sequential order at enrollment. An independently trained staff member, not otherwise involved in the study, carried out the randomization procedure using Excel. Treatment allocation was implemented using sequentially numbered, sealed, opaque envelopes. These envelopes were held by a researcher not associated with the trial. After obtaining informed consent and confirming eligibility, the treating therapist would retrieve the next envelope in sequence, open it, and apply the assigned treatment code. Each envelope also contained a unique random number that served as the patient's identifier for the duration of the study (Chen et al., 2024; Jiang et al., 2020). The assignment of participants to intervention groups, the distribution of light boxes, and the provision of instructions on how to use the boxes were conducted by non-blinded administrators. Due to the visible difference between the active and placebo devices, the intervention administrators were not blinded. The researchers responsible for clinical data collection, MRI data acquisition, and subsequent analysis were blinded to the intervention group assignments. Mood scales, MRI scans, and blood samples were collected at baseline and 8 weeks post-treatment.

2.2. Participants

Participants aged 18–28 years were recruited through advertisements at Jinan University, Guangzhou, China, between March 2020 and October 2022. All participants exhibited 2 to 4 standard depressive symptoms persisting for at least two weeks, with at least one core symptom, either a depressed mood or anhedonia. These symptoms did not follow a seasonal pattern, and Guangzhou, China, does not experience clearly defined seasonal variations. The inclusion criteria were as follows: (1) Han nationality and right-handedness; (2) 24-item Hamilton Depression Rating Scale (HAMD) score of 8–20 (Demyttenaere and De Fruyt, 2003); (3) Center for Epidemiologic Studies Depression Scale (CESD) score of $\geq$ 16 (Buntrock et al., 2016; Jiang et al., 2019); and (4) symptoms that did not have a seasonal pattern. The exclusion criteria were as follows: (1) diagnosis of major depression, bipolar disorder, schizophrenia, or other mental disorders according to the Diagnostic and Statistical Manual of Mental Disorders (DSM-5); (2) self-reported use of psychotropic interventions prior to or during the BLT; (3) presence of suicide plans or suicidal behaviors; (4) MRI contraindications; (5) current lactation or pregnancy; (6) diagnosis of other serious diseases requiring active treatment; (7) pre-existing chronic inflammatory conditions (e.g., inflammatory bowel disease, rheumatoid arthritis, or systemic inflammatory disorders).

All testing procedures were approved by the ethics committee of the First Affiliated Hospital of Jinan University (reference 2019/028) and were registered prior to the beginning of the study (trial registration: ChiCTR2000032633). All participants signed an informed consent form after receiving a complete description of the study.

2.3. Interventions

Both BLT and placebo groups utilized identical-looking custom LED (light-emitting diode) light boxes for daily 30-minute morning sessions (before 12p.m.) (Holtmann et al., 2018; Wirz-Justice et al., 2011). The active treatment device is approximately 60 cm × 30 cm × 1.5 cm in size and composed of blue-white LED (equipped with a 100% ultraviolet filter). The active treatment devices delivered light at 5000 lx intensity, while the placebo treatment device was set to emit weak light (<5 lx). The participants were instructed to position the light device on a stable surface at a fixed 50 cm distance and maintain full facial exposure without direct gaze at light source. The two switch lights were home-based use with remote monitoring (on and off) (Fig. S2). Participants in the BLT group received active treatment delivering 5000 lx light with a wavelength range of 450–700 nm, while the placebo group received light at an intensity below 5 lx. The treatment was administered once daily in 30-minute sessions over eight weeks. All participants received standardized verbal and written instructions on proper device operation.

2.4. Mood scale assessments

The HAMD and CESD were used to assess depressive symptoms (Jiang et al., 2020; Li et al., 2018; Rolle et al., 2020). Anhedonia was evaluated via the Temporal Experience of Pleasure Scale (TEPS) (Li et al., 2018). Lower TEPS scores indicate a greater level of anhedonia.

2.5. MRI data acquisition

T1 imaging, diffusion tensor imaging (DTI) and resting-state functional magnetic resonance imaging (rs-fMRI) were performed with a GE Discovery MR750 3.0 T system with an eight-channel phased array head coil (details are included in the *Supplementary Materials)*.

2.6. DTI-ALPS index analysis

DTI preprocessing was performed using tools from the FMRIB Software Library (FSL) 6.0.1 (https://fsl.fmrib.ox.ac.uk/fsl/). The DTI data underwent initial skull-stripping utilizing the Brain Extraction Tool, followed by registration to the corresponding T1 image. Subsequently, corrections for subject movement artifacts and eddy current-induced distortions were applied using the "eddy_correct" function. Diffusion tensor maps were computed using the "DTIFIT" function of FSL. Color-coded fractional anisotropy maps and diffusivity maps in the directions of the x-, y-, and z-axes (D_{xx}, D_{yy}, D_{zz}) were generated. Two neuroradiologists (with 5 and 11 years of experience) who were blinded to the patients' clinical and demographic information independently measured the regions of interest (ROIs) on the basis of the following diffusive parameters. The corona radiata projection and superior longitudinal fasciculus were used as the projection and association fibers, respectively, for DTI-ALPS index calculation (Taoka et al., 2017). The diffusivity values were registered in the x, y, and z directions for the projection fibers and association fibers, labeled D_{xxproj}, D_{yyproj}, D_{zzproj}, $D_{xxassoc}$, $D_{yyassoc}$, and $D_{zzassoc}$. All of these metrics were measured after placing a 2.5-mm radius spherical ROI in the axial slices above the bilateral ventricle body in both hemispheres according to a previous study (Carotenuto et al., 2022; Lin et al., 2023). The DTI-ALPS index was computed as ([mean(D_{xxproj}, $D_{xxassoc}$)/mean(D_{yyproj}, $D_{zzassoc}$)]) (Taoka et al., 2017). It is important to note that this index primarily reflects water diffusivity along the perivascular space, which is a constraint-based measure, rather than a direct quantification of CSF flux or clearance rate. We calculated the DTI-ALPS indices for both the left and right hemispheres, as well as the mean DTI-ALPS index for the whole brain (Fig. 2a-c).

2.7. FW analysis

A single-shell estimation model for FW was implemented utilizing the diffusion imaging in python (DIPY) software package. In this model, the signal from each voxel was fitted according to a two-compartment approach, yielding an FW map (depicting an isotropic tensor with a constant diffusion coefficient for water at body temperature) and an FW corrected tensor map (Li et al., 2024; Tang et al., 2019). The FW map indicates the proportion of FW in each voxel, varying between 0 and 1. Using this map, the average FW proportion across the white matter regions (identified by FA values below 0.2) was computed.

2.8. PVS volume analysis

The PVS volume analysis was conducted using tools from FSL 6.0.1 (https://fsl.fmrib.ox.ac.uk/fsl) (Jenkinson et al., 2012), the Advanced Normalization Tools (ANTs) software package (Avants et al., 2011), and the Quantitative Imaging Toolkit (QIT; https://github.com/cabeen/qit/). The analysis steps were as follows: 1. The images for each subject were checked for scanner artifacts and gross anatomical abnormalities. 2. An automated segmentation algorithm was employed, with which T1 images were bias-corrected. 3. Excess tissue was removed from the image, and skull stripping was performed. 4. Images were registered to Montreal Neurological Institute (MNI) 152 space via FNIRT in FSL. 5. The parcellated brain (including white matter, subcortical nuclei and the basal ganglia) was used as a mask for PVS volume quantification. 6. The Frangi filter (Frangi et al., 1998) was applied to T1 images using the QIT. 7. Optimum thresholds of 2.3 were applied to T1 images to generate a PVS map (Sepehrband et al., 2019). 8. PVS volume was normalized to the total volume of the brain regions as the percent dilated PVS (pPVS) (Chan et al., 2021).

2.9. ReHo analysis

Preprocessing was carried out with the Data Processing Assistant for Resting-State fMRI (DPABI_V3.0, http://restfmri.net/forum/DPABI) (Yan et al., 2016), which is based on Statistical Parametric Mapping (SPM12, http://www.fil.ion.ucl.ac.uk/spm/) (details are included in the *Supplementary Materials*). ReHo analysis was conducted via the DPABI software package (Yan et al., 2016). Kendall's coefficient of concordance (KCC) was computed to quantify the ReHo value, which represents the similarity of the time series of a given voxel to its 26 nearest neighboring voxels on a voxel-wise basis (Qiu et al., 2019; Zang et al., 2004). To mitigate the impact of individual variation in KCC values, normalization of the ReHo maps was performed by dividing the KCC of each voxel by the mean ReHo of the entire brain. The ReHo maps were subsequently smoothed using a Gaussian kernel with a full width at half maximum (FWHM) of 6 mm.

2.10. Pro-inflammatory cytokine measurements

Blood samples from individuals with StD were collected in the morning under fasting conditions at baseline and post-treatment, with participants abstaining from alcoholic beverages for at least one day prior to testing. Details on blood sample processing can be found in the *Supplementary Materials*. The levels of pro-inflammatory cytokines, including interleukin (IL)-1β, IL-6, IL-9, tumor necrosis factor (TNF)-α and TNF-β, in the serum were quantified with the Bio-Plex Pro Human Cytokine Assay Kit (Bio-Rad) (Chen et al., 2020).

2.11. Statistical analysis

Detailed estimations of the sample size are provided in the *Supplementary Materials*. Statistical analyses were performed using IBM SPSS Statistics 22 (Armonk, NY, USA). Demographics, mood scale scores, and cytokine levels (baseline, post-treatment, and changes from pre- to post-treatment) were compared between the BLT and placebo groups. Categorical variables were analyzed using the chi-square test. Nonparametric tests were used for nonnormally distributed data, and independent *t* tests or paired *t* tests were used for normally distributed continuous variables. Cytokine serum levels were log-transformed if they were not normally distributed.

2.11.1. Statistical analysis of the DTI-ALPS index, FW, and PVS volume

Intraclass correlation coefficients were analyzed to estimate inter-observer agreement on the DTI-ALPS index. For the DTI-ALPS index, FW and PVS volume, independent *t* tests or nonparametric tests were used to compare the metrics (baseline, post-treatment, and changes from post- to pre-treatment) between the BLT and placebo groups. The Benjamini and Hochberg false discovery rate (FDR) correction method was used for multiple comparisons. The statistical threshold was set at $p < 0.05$, two-tailed.

2.11.2. Statistical analysis of ReHo

A voxel-wise linear mixed-effects model was employed to analyze the differences in ReHo between the BLT and placebo groups (treatment × time). The linear mixed-effects model included mean frame-wise displacement as a nuisance covariate. Interaction *F*-statistic maps were corrected for multiple comparisons via Gaussian random field (GRF) correction (voxel p value < 0.005; cluster p value < 0.05). To elucidate the group differences underlying significant interaction effects, mean ReHo values were extracted from clusters identified through voxel-wise analysis with DPABI. Subsequently, ReHo values within these clusters were compared between the BLT and placebo groups at baseline and post-treatment (intergroup comparisons). Additionally, post hoc analyses were conducted to compare pre- and post-treatment ReHo values within each treatment group (intragroup comparisons).

2.11.3. Correlation analyses

When significant differences between baseline and post-treatment values were observed in the BLT group, partial correlation analysis was used to examine the correlations among the changes in the image measurements (DTI-ALPS index, PVS volume, and ReHo) (post − pre), cytokine levels (post − pre), and mood scale score improvement within groups. The nuisance covariates included in the correlation analysis were sex and age. Furthermore, multiple linear regression was used to model the relationships among changes in mood scale scores, cytokine levels, and image measurements after adjusting for potential confounders (sex and age). The significance level was set at $p < 0.05$.

3. Results

3.1. Participant characteristics and clinical symptoms

During the baseline visit, a comprehensive evaluation of 154 individuals was conducted to determine their eligibility. Of these, 137 young volunteers (89%) were selected to participate in a randomized, double-blind, placebo-controlled clinical trial. Following the acquisition of written informed consent, the eligible participants were included in the trial and randomly assigned to either the BLT group (n = 68) or the placebo group (n = 69). A total of 110 of the 137 participants (80%), comprising 57 individuals from the BLT group and 53 from the placebo group, subsequently underwent clinical assessment and MRI scanning before and after treatment. Notably, no disparities were observed in the baseline demographics or clinical characteristics between the BLT and placebo groups. Ten participants were excluded from the study because of suboptimal scan quality. Consequently, the final sample comprised 53 participants in the BLT group and 47 participants in the placebo group for the T1 images and DTI, and 47 participants in the BLT group and 42 participants in the placebo group for the rs-fMRI (Fig. 1). The demographics and treatment outcomes of the 53 participants in the BLT group and the 47 participants in the placebo group are shown in Table 1. A concise summary illustrating the study design along with the key findings is depicted in Fig. S1.

Compared with the placebo group, the BLT group showed significant relief in HAMD scores ($t = 3.576$, FDR-$p = 0.002$), CESD scores ($t = 3.520$, FDR-$p = 0.002$), and TEPS scores ($t = 2.333$, FDR-$p = 0.022$) from baseline to post-treatment (Table S1 and Fig. S3).

The magnitude of improvement was quantified using effect sizes. The between-group effect size (Cohen's *d*) for the reduction in HAMD scores was 0.56 (95% CI: 0.17 to 0.95), indicating a moderate effect favoring BLT over placebo. Similarly, the effect sizes for CESD and TEPS scores were 0.69 (95% CI: 0.29 to 1.08) and 0.46 (95% CI: 0.05 to 0.87), respectively.

3.2. DTI-ALPS index, FW and PVS volume

The apparent diffusion coefficient and DTI-ALPS index were in good agreement between the two radiologists (intraclass correlation coefficient, 0.90 [95% CI: 0.85, 0.93]) (Table S2). No significant difference was observed in the baseline DTI-ALPS indices between the BLT and placebo groups. After treatment, compared with the placebo group, the BLT group showed a significant increase in the mean DTI-ALPS index ($t = 3.765$, FDR-$p < 0.001$), left DTI-ALPS index ($t = 2.928$, FDR-$p = 0.004$), and right DTI-ALPS index ($t = 3.746$, FDR-$p < 0.001$) (Table 2 and Fig. 2d-f). Similarly, the BLT group exhibited significantly greater changes from baseline in the mean DTI-ALPS index ($t = 2.585$, FDR-$p = 0.026$), left DTI-ALPS index ($t = 2.261$, FDR-$p = 0.026$), and right DTI-ALPS index ($t = 2.334$, FDR-$p = 0.026$) compared to the placebo group (Table 2 and Fig. 2d-f).

No significant differences in white matter FW changes were observed between the two groups. However, paired *t* tests within the BLT group indicated a significant FW reduction ($t = -2.248$, $p = 0.029$) (Table 2, Table S3, and Fig. S4a), whereas no such reduction was found in the placebo group.

No significant difference was observed in baseline, post-treatment, or changes from pre- to post-treatment pPVS within the white matter, subcortical regions, or basal ganglia between the BLT and placebo groups (Table 2).

3.3. ReHo analysis

There were significant interactions between treatment and time in the ReHo of the left superior frontal gyrus (SFG) (peak MNI = −15, 15, 57, $F = 19.298$, $p < 0.001$, 31 voxels) (Table S4 and Fig. 3). Post hoc analyses indicated that, compared with the placebo group ($t = -4.166$, $p < 0.001$), the BLT group had lower ReHo in the left SFG at baseline, and no differences were observed between the two groups at post-treatment ($t = 1.447$, $p = 0.151$). Moreover, compared with the baseline values, ReHo was increased post-treatment in the left SFG of participants in the BLT group ($t = 4.868$, $p < 0.001$). Conversely, decreased ReHo in the left SFG was detected post-treatment compared with baseline in the placebo group ($t = -2.423$, $p = 0.020$).

3.4. Serum pro-inflammatory cytokines

Blood samples from 72 subjects (N = 36 and N = 36 in the BLT and placebo groups, respectively) were obtained for analyses (Table S5). Changes in pro-inflammatory cytokine levels were evaluated as exploratory outcomes. No significant differences in the changes in pro-inflammatory cytokine levels were found between the two groups. However, Wilcoxon signed-rank tests within the BLT group revealed a

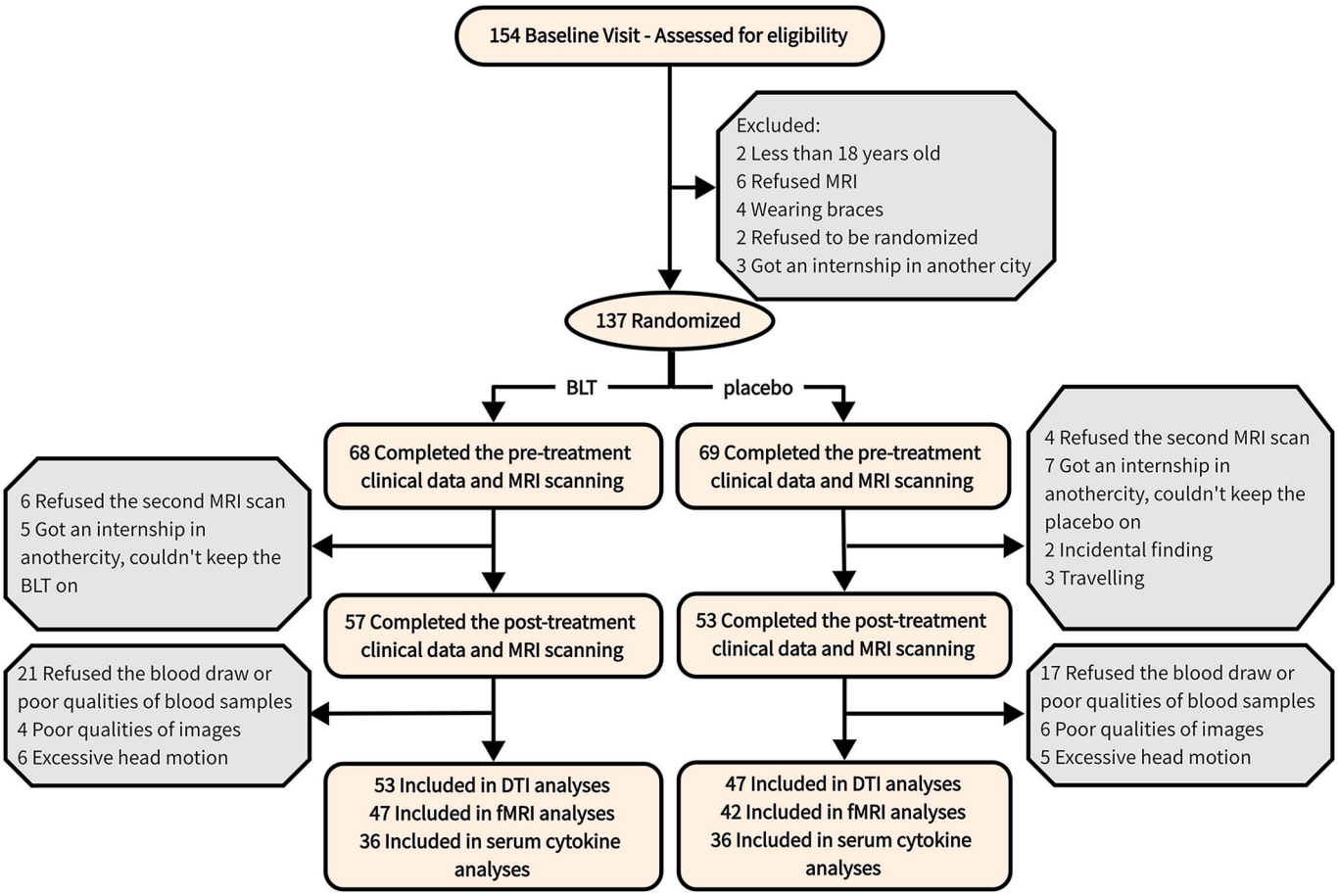

Fig. 1. Flow chart of participants throughout the study, from the initial eligibility assessment to the final analyses. BLT, bright light therapy; MRI, magnetic resonance imaging; DTI, diffusion tensor imaging; fMRI, functional MRI.

significant reduction in IL-9 and TNF-β (z = -2.388, p = 0.017; z = -2.596, p = 0.009) levels after log transformation, which was not observed in the placebo group (Fig. S4b-c).

3.5. Correlations among changes in image measurements, cytokine levels, and mood scale scores

A significant correlation was observed between the changes in TEPS scores and the changes in the right DTI-ALPS index (r = 0.286, p = 0.042) in the BLT group (Fig. 4a). Significant correlations were observed between the changes in the ReHo value of the left SFG and the changes in the mean and left DTI-ALPS indices (r = 0.305p = 0.042; r = 0.413, p = 0.005) in the BLT group (Fig. 4b-c). Significant correlations were observed between the changes in IL-9 levels (when log-transformed) and changes in the mean and right DTI-ALPS indices (r = 0.385, p = 0.036; r = 0.393, p = 0.032), as well as between changes in TNF-β levels (when log-transformed) and changes in the right DTI-ALPS index (r = 0.362, p = 0.049) in the BLT group (Fig. 4d-f). There were no significant correlations among any of the changes in image measurements, cytokine levels, or mood scale scores in the placebo group ($p > 0.05$).

Multiple regression analysis demonstrated that the interaction of changes in the mean DTI-ALPS index × changes in the ReHo value of the left SFG (β = -38.730, t = -2.122, p = 0.040) was an independent predictor of changes in the TEPS score in the BLT group. Multiple regression analysis also demonstrated that the interaction of changes in the left DTI-ALPS index × changes in the TNF-β level (β = 282.560, t = 2.418, p = 0.023) was an independent predictor of changes in the CESD score in the BLT group. The interaction effect of changes in the TNF-β level × changes in the white matter FW (β = -76.206, t = -2.721, p = 0.013) was an independent predictor of changes in the TEPS score in the BLT group. The interaction effect of changes in the IL-9 level × changes in the ReHo value of the left SFG (β = -76.206, t = -2.721, p = 0.013) was an independent predictor of changes in the HAMD score in the BLT group. In the placebo group, there were no relationships among changes in mood scale scores, cytokine levels, or image measurements ($p > 0.05$).

4. Discussion

This study is the first to evaluate the effects of light therapy on brain glymphatic function in individuals with StD. The major findings in individuals with StD were as follows: (1) BLT increased the DTI-ALPS index values and reduced the amount of FW; (2) BLT increased ReHo in the left SFG; (3) BLT decreased the IL-9 and TNF-β levels; and (4) the altered DTI-ALPS index was associated with improved depressive symptoms, increased ReHo in the SFG, and decreased levels of pro-inflammatory cytokines in the BLT group.

4.1. Effects of BLT on glymphatic function

Compared with the placebo, BLT significantly elevated the DTI-ALPS index values and reduced the amount of FW in individuals with StD. Moreover, a significant positive correlation was observed between the changes in TEPS scores and the changes in the right DTI-ALPS index in the BLT group. Anhedonia, or loss of interest or pleasure in usual activities, is a hallmark symptom of depression and is highly prevalent among individuals with mood disorders. These findings suggest that light exposure may influence glymphatic system activity in participants with StD. In animal models of depression, such as the chronic

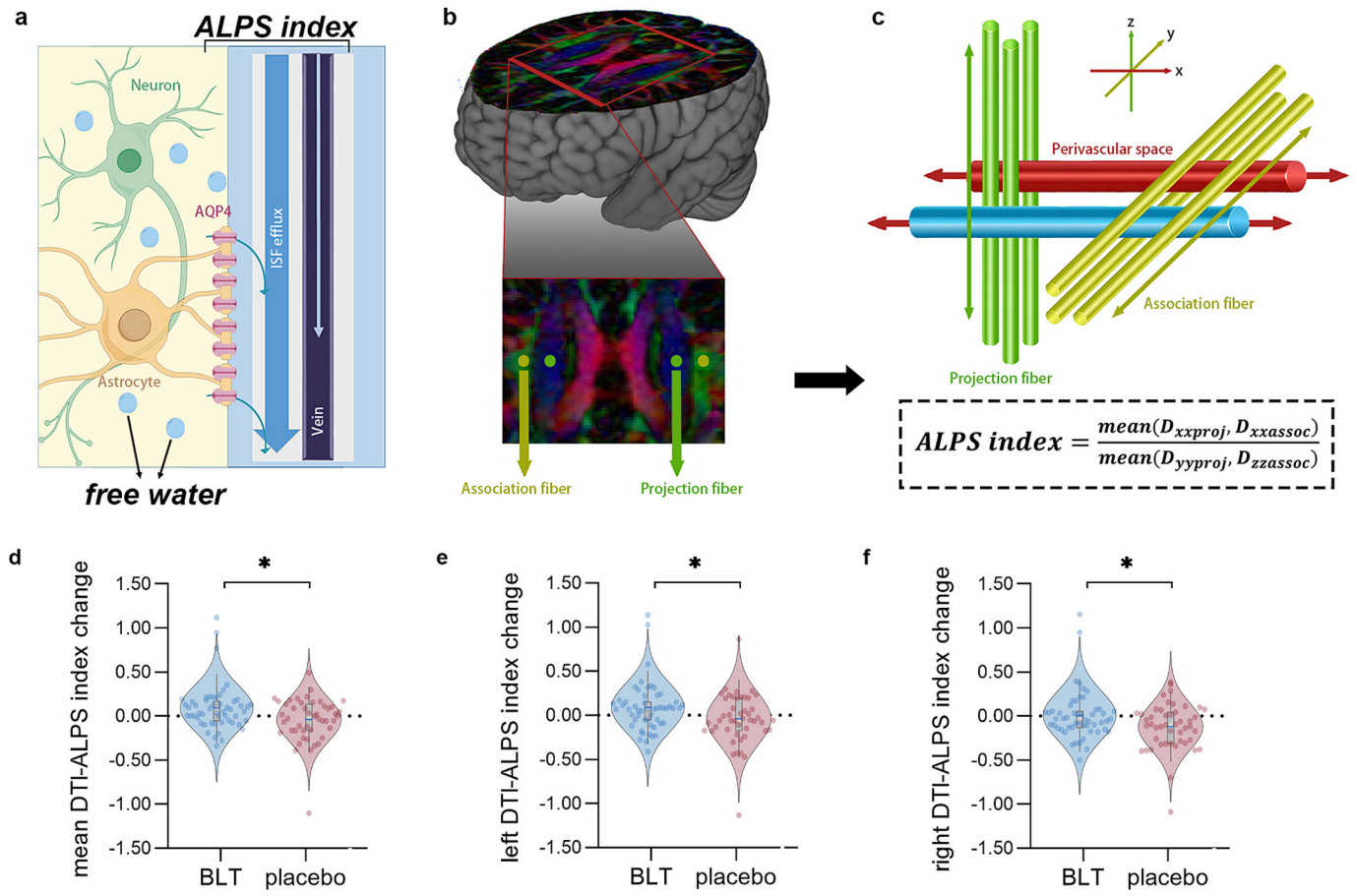

Fig. 2. Flowchart of DTI-ALPS index calculation and comparison of the DTI-ALPS indices at baseline and post-treatment in both the BLT and placebo groups. (a) Diagram of the essential physiologic activities in PVS network circulation. (b) On the color-coded FA map, spherical ROIs were placed in the association and projection areas at the level of the lateral ventricle. (c) Relationship between the perivascular space and the directions of the association and projection fibers. The Dominant fibers within the association area predominantly align along the y-axis, perpendicular to both the x- and z-axes, whereas the dominant fibers within the projection area align along the z-axis, perpendicular to both the x- and y-axes. The DTI-ALPS index was calculated via the tensor map (D_{xx}, D_{yy}, and D_{zz}) with the sphere ROIs. (d-f) Group comparison of DTI-ALPS index change. DTI-ALPS, diffusion tensor image analysis along the perivascular space; BLT, bright light therapy; PVS, perivascular space; ISF, parenchymal interstitial fluid; AQP4, aquaporin DTI-ALPS, diffusion tensor image analysis along the perivascular space. The *p*-values for changes in the DTI-ALPS indices were obtained using independent-sample *t*-tests. *, $p < 0.05$, **, $p < 0.01$, ***, $p < 0.001$.

Table 1
Participant demographics and comparison of mood scale scores between the BLT and placebo groups.

	BLT	Placebo	$t/x^2/z$	*P*
Number of participants	53	47	–	–
Sex (male/female)	20/33	15/32	0.371	0.542†
Age (years)	23.40 (2.47)	22.81 (2.36)	1.212	0.228[a]
Education (years)	17.06 (2.11)	16.77 (1.97)	0.710	0.479[a]
Baseline HAMD	14.40(3.87)	15.60(3.63)	−1.593	0.114[a]
Baseline CESD	27.36(8.06)	28.79(7.56)	−0.911	0.365[a]
Baseline TEPS	68.36 (13.31)	67.28 (12.22)	0.423	0.673[a]
Post-treatment HAMD	6.74(4.39)	10.72(6.65)	−3.576	0.001[a,**]
Post-treatment CESD	15.43(6.51)	23.62 (10.50)	−4.740	< 0.001[a,***]
Post-treatment TEPS	76.23 (11.90)	71.49 (11.59)	2.013	0.047[a,*]
Relief in HAMD	7.66(4.74)	4.87(5.22)	2.801	0.006[a,**]
Relief in CESD	11.92(9.49)	5.17(10.20)	3.429	0.001[a,**]
Relief in TEPS	7.87(11.30)	3.46(7.32)	2.267	0.026[a,*]

Mean (standard deviation) or median (interquartile range) is reported unless otherwise noted. BLT, bright light therapy; HAMD, Hamilton Depression Rating Scale; CESD, Centre for Epidemiologic Studies Depression Scale; TEPS, the Temporal Experience of Pleasure Scale. †, The *p* value for gender distribution was obtained by chi-square test. [a], The *p* values were obtained by independent-sample *t*-tests. *, $p < 0.05$, **, $p < 0.01$, ***, $p < 0.001$.

unavoidable mild stress (CUMS) model, glymphatic system function is disrupted, which is correlated with behavioral manifestations of depression (including anhedonia) and cognitive impairment (X. H. Liu et al., 2020; Xia et al., 2017; Yao et al., 2023). A previous study revealed that CUMS slowed the clearance function of the glymphatic system, leading to Aβ42 accumulation in the brain parenchyma, but treatment with the antidepressant fluoxetine reversed these destructive effects (Xia et al., 2017). Another study revealed that melatonin ameliorated depressive symptoms in model mice by regulating the expression of the circadian protein Per2, maintaining the circadian rhythm of astrocytic AQP4 polarization, and restoring glymphatic function (Yao et al., 2023). Previous work in both humans and animal models has shown that light therapy modulates melatonin rhythms in circadian and mood disorders (Pail et al., 2011; Thalén et al., 1995). A recent study revealed that flickering light at 40 Hz bolstered glymphatic influx and efflux in mice by increasing astrocytic AQP4 polarization and enhancing vasomotion (Sun et al., 2024b). Therefore, we speculated that BLT may influence the underlying glymphatic system activity, thereby improving depressive symptoms, especially anhedonia.

4.2. *Effects of BLT on brain functional activity*

Another major result of this study was a significant increase in ReHo in the left SFG following the 8-week BLT treatment in StD. Altered ReHo

Table 2
Comparison of glymphatic function between the BLT and placebo groups.

	BLT	Placebo	$t/x^2/z$	*P*
Baseline mean DTI-ALPS	1.73 (0.29)	1.70 (0.16)	0.690	0.492[a]
Baseline L DTI-ALPS	1.73 (0.30)	1.71 (0.21)	0.264	0.792[a]
Baseline R DTI-ALPS	1.73 (0.31)	1.68 (0.20)	0.963	0.338[a]
Post-treatment mean DTI-ALPS	1.81 (0.20)	1.65 (0.23)	3.765	< 0.001[a,***]
Post-treatment L DTI-ALPS	1.82 (0.23)	1.67 (0.25)	2.928	0.004[a,**]
Post-treatment R DTI-ALPS	1.81 (0.22)	1.62 (0.27)	3.746	< 0.001[a,***]
Change in mean DTI-ALPS	0.08 (0.26)	−0.05 (0.25)	2.585	0.011[a,*]
Change in L DTI-ALPS	0.09 (0.28)	−0.04 (0.29)	2.261	0.027[a,*]
Change in R DTI-ALPS	0.08 (0.30)	−0.06 (0.28)	2.334	0.022[a,*]
Baseline FW	0.342 (0.013)	0.341 (0.008)	0.598	0.551[a]
Post-treatment FW	0.339 (0.011)	0.340 (0.009)	−0.008	0.994[a]
Change in FW	−0.002 (0.008)	−0.001 (0.006)	−0.921	0.359[a]
Baseline WM-pPVS	0.194 (0.180–0.209)	0.187 (0.179–0.203)	1.563	0.118[b]
Baseline subcortical pPVS	0.148 (0.142–0.158)	0.150 (0.141–0.158)	−0.049	0.961[b]
Baseline BG-pPVS	0.055 (0.049–0.061)	0.056 (0.052–0.061)	−0.596	0.551[b]
Post-treatment WM-pPVS	0.195 (0.178–0.209)	0.190 (0.178–0.203)	0.967	0.334[b]
Post-treatment subcortical pPVS	0.151 (0.141–0.162)	0.149 (0.142–0.156)	0.925	0.355[b]
Post-treatment BG-pPVS	0.052 (0.048–0.061)	0.056 (0.049–0.062)	−1.191	0.234[b]
Change in WM-pPVS	−0.003 (−0.008–0.007)	−0.001 (−0.008–0.010)	−0.750	0.453[b]
Change in subcortical pPVS	< −0.001 (−0.006–0.010)	0.001 (−0.012–0.006)	−0.743	0.458[b]
Change in BG-pPVS	< −0.001 (−0.006–0.005)	−0.001 (−0.003–0.006)	−0.540	0.590[b]

Mean (standard deviation) or median (interquartile range) is reported unless otherwise noted. BLT, bright light therapy; DTI-ALPS, diffusion tensor image analysis along the perivascular space; FW, free water; pPVS, percent perivascular space; WM-pPVS, percent perivascular space of white matter; BG-pPVS, percent perivascular space of basal ganglia. †, The *p* value for gender distribution was obtained by chi-square test. [a], The *p* values were obtained by independent-sample *t*-tests. [b], The *p* values were obtained by nonparametric tests. *, $p < 0.05$, **, $p < 0.01$, ***, $p < 0.001$.

in the SFG was positively correlated with an increased DTI-ALPS index in the BLT group, suggesting a potential link between brain functional activity and the glymphatic system. Additionally, the interaction effect of changes in the ReHo × DTI-ALPS index was correlated with reduced anhedonia in BLT-treated subjects with StD. Numerous preclinical and clinical investigations have identified both structural and functional abnormalities in the prefrontal cortex associated with depression (Gong et al., 2020; Pizzagalli and Roberts, 2022). In addition, several studies on anhedonia have focused mainly on deficits in frontostriatal reward processing circuitry (Der-Avakian and Markou, 2012). A previous task-based fMRI study revealed decreased activity in the left SFG during negative emotion processing in individuals with StD (Zhang et al., 2022b). Our recent study reported that BLT increased the functional connectivity between the midbrain and SFG (Chen et al., 2024). Similarly, Alkozei et al. (Alkozei et al., 2016) reported that short exposure to blue light increased activation in the ventrolateral and dorsolateral prefrontal cortex in healthy participants during working memory tasks (Alkozei et al., 2016). Therefore, these findings indicate an increase in spontaneous neural activity in the prefrontal cortex after light therapy in individuals with StD. Neural activity has also been shown to correlate with CSF flow in mice and humans (Williams et al., 2023b). A previous study demonstrated that lower DTI-ALPS indices were associated with smaller gray matter volumes in several brain regions involved in cognitive function (e.g., the frontal cortex, hippocampus, and thalamus) in community-dwelling older adults, suggesting that these areas are vulnerable to glymphatic dysfunction (Siow et al., 2022). Therefore, we speculated that altering glymphatic system function may augment spontaneous neural activity in the prefrontal cortex after BLT treatment for StD.

4.3. *Effects of BLT on inflammation*

In addition, BLT decreased the levels of the peripheral pro-inflammatory cytokines IL-9 and TNF-β in individuals with StD, suggesting that BLT affects the inflammatory response in depression. Exploratory analyses indicated that altered serum IL-9 and TNF-β levels were positively correlated with changes in the DTI-ALPS index in the BLT group. The effect of BLT on inflammation has been investigated in few studies. A previous study revealed that combining BLT with oral antidepressants altered the levels of inflammatory markers (e.g., decreased neutrophil/lymphocyte ratio) in patients with nonseasonal depression (Demirkol et al., 2019). A recent animal study revealed that BLT reduced the levels of pro-inflammatory markers in corticolimbic brain regions in a diurnal rodent model of seasonal affective disorder (Costello et al., 2023). Recent evidence from depression research indicates that blood–brain barrier disruption and elevated inflammatory cytokine levels in states of persistent stress or trauma may contribute to the development of symptoms (Medina-Rodriguez and Beurel, 2022). Excessive inflammation may induce vascular dysfunction, thereby impairing glymphatic system function. Conversely, dysfunction of the glymphatic system can result in substantial accumulation of proteins and waste products, which in turn may provoke inflammatory responses (Cai et al., 2024). A preclinical study revealed that polyunsaturated fatty acid supplementation alleviated depression-like behaviors in mice, reduced neuroinflammation and cerebrovascular dysfunction, and ultimately improved cognitive performance, all of which were accompanied by the restoration of glymphatic system function (Liu et al., 2020). Taken together, these findings suggest a possible association between decreased inflammation and enhanced glymphatic system function in individuals with depression following light therapy.

There are several limitations in this study. First, this study did not include the use of intrathecal contrast medium-enhanced MRI for individuals with StD, despite its current recognition as the gold standard for assessing glymphatic system function. We relied instead on indirect, non-invasive indices (DTI-ALPS, PVS, and FW). Additionally, the observed changes may be confounded by other physiological factors, including cerebral blood flow alterations or general fluid shifts (Ghaderi et al., 2025). Second, this study relied on a limited set of peripheral cytokines, which may not accurately reflect neuroinflammation within the central nervous system. Third, given that our study is exploratory, the findings from the correlation analysis should be interpreted with caution, as the results cannot survive multiple comparison corrections. Fourth, the unequal attrition across groups, despite efforts to retain participants, could compromise the interpretation of efficacy outcomes by introducing potential bias. Sixth, treatment compliance cannot be confirmed with BLT. Despite this, we monitored the status of the light device (on and off) to ensure adherence of the participants. When the light device was off, we reminded the participants to turn on the device, encouraging compliance. Finally, the lack of long-term follow-up and the use of a homogeneous sample (young, right-handed, comorbidity-free Han Chinese students) limit conclusions on effect durability and generalizability. As such, replication in more diverse, multi-center

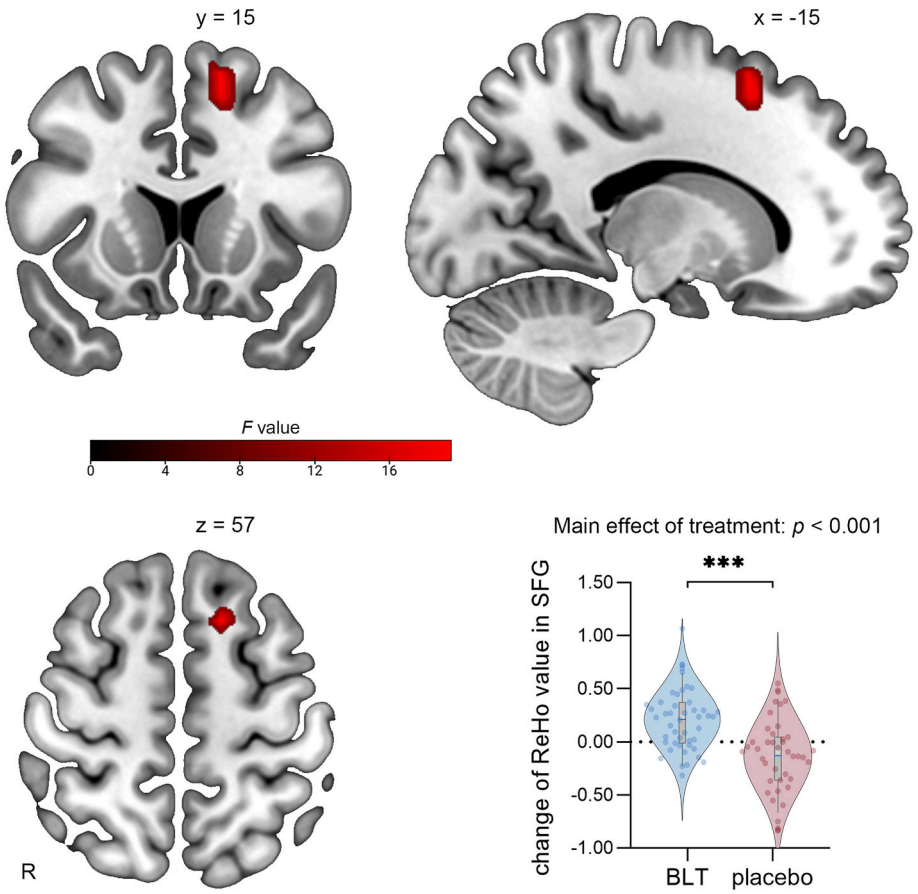

Fig. 3. Group comparisons of ReHo: whole-brain analysis and ReHo change in the left SFG (BLT vs. placebo). ReHo, regional homogeneity; BLT, bright light therapy; SFG, superior frontal gyrus; L, left; R, right.

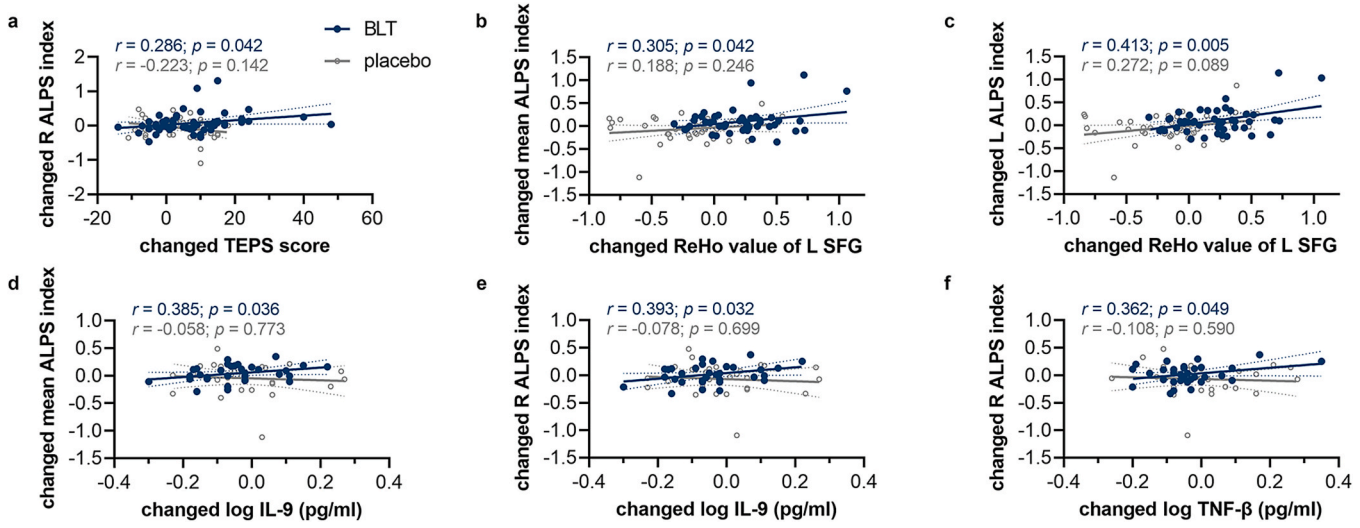

Fig. 4. Correlations between changes in images, changes in cytokines, and changes in mood scale scores. (a) Correlations between changes in the TEPS score and changes in the right DTI-ALPS index. (b-c) Correlations between changes in the ReHo value of the left SFG and changes in the mean/left DTI-ALPS index. (d-f) Correlations between changes in IL-9 levels (log-transformed) and changes in the mean/right DTI-ALPS index, as well as between changes in TNF-β levels (log-transformed) and changes in the right DTI-ALPS index. DTI-ALPS, diffusion tensor image analysis along the perivascular space. BLT, bright light therapy; TEPS, Temporal Experience of Pleasure Scale; IL-9, interleukin-9; TNF-β, tumor necrosis factor-beta; log, natural log. ReHo, regional homogeneity; SFG, superior frontal gyrus; L, left; R, right.

populations with extended follow-up is warranted in future research.

5. Conclusions

In conclusion, BLT influences glymphatic system function in

individuals with StD. Moreover, the enhancement of glymphatic function is associated with reduced inflammation, enhanced functional activity of the prefrontal cortex, and alleviation of depressive symptoms.

CRediT authorship contribution statement

Pan Chen: Writing – review & editing, Writing – original draft, Visualization, Validation, Supervision, Software, Resources, Project administration, Methodology, Investigation, Formal analysis, Data curation. **Guanmao Chen:** Writing – review & editing, Validation, Software, Resources, Project administration, Methodology, Investigation, Formal analysis, Data curation, Conceptualization. **Zixuan Guo:** Writing – original draft, Supervision, Software, Project administration, Methodology, Investigation, Formal analysis. **Ruoyi Chen:** Visualization, Validation, Software, Resources, Formal analysis. **Xinyue Tang:** Validation, Software, Data curation. **Zibin Yang:** Formal analysis, Data curation. **Wenhao Ma:** Supervision, Data curation. **Chao Chen:** Formal analysis. **Shilin Sun:** Data curation. **Yuan Zhang:** Formal analysis, Data curation. **Hui Zhong:** Supervision, Software, Project administration. **Shu Zhang:** Data curation. **Zhangzhang Qi:** Data curation. **Wenjie Fang:** Data curation. **Lijun Jiang:** Data curation. **Zhinan Yin:** Conceptualization. **Li Huang:** Conceptualization. **Junxian Ma:** Conceptualization. **Qian Tao:** Writing – review & editing, Resources, Funding acquisition, Data curation. **Ying Wang:** Writing – review & editing, Writing – original draft, Supervision, Resources, Project administration, Methodology, Funding acquisition, Data curation, Conceptualization.

Declaration of competing interest

The authors declare that they have no known competing financial interests or personal relationships that could have appeared to influence the work reported in this paper.

Acknowledgments

The study was supported by grants from the National Natural Science Foundation of China (82472057, 81971597), Science and Technology Projects in Guangzhou (2024B03J1299). The funding organizations play no further role in study design, data collection, analysis and interpretation and paper writing.

Appendix A. Supplementary data

Supplementary data to this article can be found online at https://doi.org/10.1016/j.bbi.2026.106484.

Data availability

Data will be made available on request.

References

Alkozei, A., Smith, R., Pisner, D.A., Vanuk, J.R., Berryhill, S.M., Fridman, A., Killgore, W. D., 2016. Exposure to blue light increases subsequent functional activation of the prefrontal cortex during performance of a working memory task. Sleep 39, 1671–1680.

Avants, B.B., Tustison, N.J., Wu, J., Cook, P.A., Gee, J.C., 2011. An open source multivariate framework for n-tissue segmentation with evaluation on public data. Neuroinformatics 9, 381–400.

Bae, Y.J., Kim, J.M., Choi, B.S., Ryoo, N., Song, Y.S., Nam, Y., Kim, J.H., 2023. Altered brain glymphatic flow at diffusion-tensor MRI in rapid eye movement sleep behavior disorder. Radiology 307.

Bissig, D., Zhou, C.G., Le, V., Bernard, J.T., 2020. Optical coherence tomography reveals light-dependent retinal responses in Alzheimer's disease. Neuroimage 219, 117022.

Bohr, T., Hjorth, P.G., Holst, S.C., Hrabetová, S., Kiviniemi, V., Lilius, T., Nedergaard, M., 2022. The glymphatic system: Current understanding and modeling. Iscience, 25.

Buntrock, C., Ebert, D.D., Lehr, D., Smit, F., Riper, H., Berking, M., Cuijpers, P., 2016. Effect of a web-based guided self-help intervention for prevention of major depression in adults with subthreshold depression: a randomized clinical trial. J. Am. Med. Assoc. 315, 1854–1863.

Cai, Y., Zhang, Y.Q.Q., Leng, S., Ma, Y.Y., Jiang, Q., Wen, Q.T., Hu, J.N., 2024. The relationship between inflammation, impaired glymphatic system, and neurodegenerative disorders: a vicious cycle. Neurobiol. Dis. 192, 16.

Carotenuto, A., Cacciaguerra, L., Pagani, E., Preziosa, P., Filippi, M., Rocca, M.A., 2022. Glymphatic system impairment in multiple sclerosis: relation with brain damage and disability. Brain 145, 2785–2795.

Chan, S.T., Mercaldo, N.D., Ravina, B., Hersch, S.M., Rosas, H.D., 2021. Association of dilated perivascular spaces and disease severity in patients with huntington disease. Neurology 96, e890–e894.

Chen, G.M., Chen, P., Yang, Z.B., Ma, W.H., Yan, H., Su, T., Wang, Y., 2024. Increased functional connectivity between the midbrain and frontal cortex following bright light therapy in subthreshold depression: a randomized clinical trial. Am. Psychol. 79, 437–450.

Chen, P., Chen, F., Chen, G., Zhong, S., Gong, J., Zhong, H., Wang, Y., 2020. Inflammation is associated with decreased functional connectivity of insula in unmedicated bipolar disorder. Brain Behav. Immun. 89, 615–622.

Costello, A., Linning-Duffy, K., Vandenbrook, C., Lonstein, J.S., Yan, L., 2023. Effects of bright light therapy on neuroinflammatory and neuroplasticity markers in a diurnal rodent model of seasonal affective disorder. Ann. Med. 55.

Cuijpers, P., Koole, S.L., van Dijke, A., Roca, M., Li, J., Reynolds 3rd., C.F., 2014. Psychotherapy for subclinical depression: meta-analysis. Br. J. Psychiatry 205, 268–274.

Cuijpers, P., Pineda, B.S., Ng, M.Y., Weisz, J.R., Muñoz, R.F., Gentili, C., Karyotaki, E., 2021. A meta-analytic review: psychological treatment of subthreshold depression in children and adolescents. J. Am. Acad. Child Adolesc. Psychiatry 60, 1072–1084.

de Almeida, A.M., de Moraes, F.C.A., Souza, M.E.C., Cardoso, J., Tamashiro, F., Miranda, C., Kelly, F.A., 2025. Bright light therapy for nonseasonal depressive disorders: a systematic review and meta-analysis. JAMA Psychiat. 82, 38–46.

Demirkol, M.E., Namli, Z., Tamam, L., 2019. Efficacy of light therapy on non-seasonal depression and inflammatory markers. Eur. J. Psych. 33, 104–111.

Demyttenaere, K., De Fruyt, J., 2003. Getting what you ask for: on the selectivity of depression rating scales. Psychother. Psychosom. 72, 61–70.

Der-Avakian, A., Markou, A., 2012. The neurobiology of anhedonia and other reward-related deficits. Trends Neurosci. 35, 68–77.

Frangi, A.F., Niessen, W.J., Vincken, K.L., Viergever, M.A., 1998. Multiscale vessel enhancement filtering. In: Wells, W.M., Colchester, A., Delp, S. (Eds.), Medical Image Computing and Computer-Assisted Intervention - Miccai'98, Vol. 1496. Springer-Verlag, Berlin, Berlin, pp. 130–137.

Geoffroy, P.A., Schroder, C.M., Reynaud, E., Bourgin, P., 2019. Efficacy of light therapy versus antidepressant drugs, and of the combination versus monotherapy, in major depressive episodes: a systematic review and meta-analysis. Sleep Med. Rev. 48, 101213.

Ghaderi, S., Mohammadi, S., Jouzdani, A.F., Ahmadzadeh, A.M., Fatehi, F., 2025. A systematic review and meta-analysis on glymphatic flow dysfunction in Parkinson's disease and Parkinsonism spectrum. NPJ Parkinsons Dis. 11, 306.

Gong, J.Y., Wang, J.J., Qiu, S.J., Chen, P., Luo, Z.Y., Wang, J.R., Wang, Y., 2020. Common and distinct patterns of intrinsic brain activity alterations in major depression and bipolar disorder: voxel-based meta-analysis. Transl. Psychiatry 10.

Holtmann, M., Mokros, L., Kirschbaum-Lesch, I., Kölch, M., Plener, P.L., Ruckes, C., Legenbauer, T., 2018. Adolescent depression: Study protocol for a randomized, controlled, double-blind multicenter parallel group trial of bright light therapy in a naturalistic inpatient setting (DeLight). Trials 19, 568.

Iliff, J.J., Wang, M., Liao, Y., Plogg, B.A., Peng, W., Gundersen, G.A., Nedergaard, M., 2012. A paravascular pathway facilitates CSF flow through the brain parenchyma and the clearance of interstitial solutes, including amyloid β. Sci. Transl. Med. 4, 147ra111.

Jenkinson, M., Beckmann, C.F., Behrens, T.E., Woolrich, M.W., Smith, S.M., 2012. Fsl. Neuroimage 62, 782–790.

Jiang, L., Wang, Y., Zhang, Y., Li, R., Wu, H., Li, C., Tao, Q., 2019. The reliability and validity of the center for epidemiologic studies depression scale (CES-D) for Chinese university students. Front. Psych. 10, 315.

Jiang, L., Zhang, S., Wang, Y., So, K.F., Ren, C., Tao, Q., 2020. Efficacy of light therapy for a college student sample with non-seasonal subthreshold depression: an RCT study. J. Affect. Disord. 277, 443–449.

Jiang, X., Luo, Y., Chen, Y., Yan, J., Xia, Y., Yao, L., Chen, Y., 2021. Comparative efficacy of multiple therapies for the treatment of patients with subthreshold depression: a systematic review and network meta-analysis. Front. Behav. Neurosci. 15, 755547.

Kamagata, K., Andica, C., Takabayashi, K., Saito, Y., Taoka, T., Nozaki, H., Neuroimaging, A.D., 2022. Association of MRI indices of glymphatic system with amyloid deposition and cognition in mild cognitive impairment and alzheimer disease. Neurology 99, E2648–E2660.

Lam, R.W., Levitt, A.J., Levitan, R.D., Michalak, E.E., Cheung, A.H., Morehouse, R., Tam, E.M., 2016. Efficacy of bright light treatment, fluoxetine, and the combination in patients with nonseasonal major depressive disorder: a randomized clinical trial. JAMA Psychiat. 73, 56–63.

Li, H., Jacob, M.A., Cai, M., Kessels, R.P.C., Norris, D.G., Duering, M., Tuladhar, A.M., 2024. Perivascular spaces, diffusivity along perivascular spaces, and free water in cerebral small vessel disease. Neurology 102, e209306.

Li, Z., Shi, H.S., Elis, O., Yang, Z.Y., Wang, Y., Lui, S.S.Y., Chan, R.C.K., 2018. The structural invariance of the temporal experience of pleasure scale across time and culture. Psych J 7, 59–67.

Lin, L.P., Su, S., Hou, W., Huang, L., Zhou, Q., Zou, M., Chen, Y., 2023. Glymphatic system dysfunction in pediatric acute lymphoblastic leukemia without clinically

diagnosed central nervous system infiltration: a novel DTI-ALPS method. Eur. Radiol. 33, 3726–3734.
Lin, S., Lin, X., Chen, S., Liang, Q., Li, Y., Wei, F., Qiu, Y., 2024. Association of MRI indexes of the perivascular space network and cognitive impairment in patients with obstructive sleep apnea. Radiology 311, e232274.
Liu, S.W., Sun, X.H., Ren, Q.G., Chen, Y.J., Dai, T.J., Yang, Y.R., Yan, C.Z., 2024. Glymphatic dysfunction in patients with early-stage amyotrophic lateral sclerosis. Brain 147, 100–108.
Liu, X.H., Hao, J.H., Yao, E.S., Cao, J., Zheng, X.L., Yao, D., Wang, W., 2020. Polyunsaturated fatty acid supplement alleviates depression-incident cognitive dysfunction by protecting the cerebrovascular and glymphatic systems. Brain Behav. Immun. 89, 357–370.
Lohela, T.J., Lilius, T.O., Nedergaard, M., 2022. The glymphatic system: implications for drugs for central nervous system diseases. Nat. Rev. Drug Discov. 21, 763–779.
Medina-Rodriguez, E.M., Beurel, E., 2022. Blood brain barrier and inflammation in depression. Neurobiol. Dis. 175.
Murdock, M.H., Yang, C.Y., Sun, N., Pao, P.C., Blanco-Duque, C., Kahn, M.C., Tsai, L.H., 2024. Multisensory gamma stimulation promotes glymphatic clearance of amyloid. Nature 627, 149–156.
Nedergaard, M., Goldman, S.A., 2020. Glymphatic failure as a final common pathway to dementia. Science 370, 50-+.
Pail, G., Huf, W., Pjrek, E., Winkler, D., Willeit, M., Praschak-Rieder, N., Kasper, S., 2011. Bright-light therapy in the treatment of mood disorders. Neuropsychobiology 64, 152–162.
Pizzagalli, D.A., Roberts, A.C., 2022. Prefrontal cortex and depression. Neuropsychopharmacology 47, 225–246.
Qiu, S., Chen, F., Chen, G., Jia, Y., Gong, J., Luo, X., Wang, Y., 2019. Abnormal resting-state regional homogeneity in unmedicated bipolar II disorder. J. Affect. Disord. 256, 604–610.
Rasmussen, M.K., Mestre, H., Nedergaard, M., 2018. The glymphatic pathway in neurological disorders. Lancet Neurol. 17, 1016–1024.
Rohan, K.J., Mahon, J.N., Evans, M., Ho, S.Y., Meyerhoff, J., Postolache, T.T., Vacek, P. M., 2015. Randomized trial of cognitive-behavioral therapy versus light therapy for seasonal affective disorder: acute outcomes. Am. J. Psychiatry 172, 862–869.
Rolle, C.E., Fonzo, G.A., Wu, W., Toll, R., Jha, M.K., Cooper, C., Etkin, A., 2020. Cortical connectivity moderators of antidepressant vs placebo treatment response in major depressive disorder secondary analysis of a randomized clinical trial. JAMA Psychiat. 77, 397–408.
Salehpour, F., Khademi, M., Bragin, D.E., DiDuro, J.O., 2022. Photobiomodulation therapy and the glymphatic system: promising applications for augmenting the brain lymphatic drainage system. Int. J. Mol. Sci. 23.
Sepehrband, F., Barisano, G., Sheikh-Bahaei, N., Cabeen, R.P., Choupan, J., Law, M., Toga, A.W., 2019. Image processing approaches to enhance perivascular space visibility and quantification using MRI. Sci. Rep. 9, 12351.
Shen, T., Yue, Y., Ba, F., He, T., Tang, X., Hu, X., Lai, H.Y., 2022. Diffusion along perivascular spaces as marker for impairment of glymphatic system in Parkinson's disease. NPJ Parkinsons Dis 8, 174.
Siow, T.Y., Toh, C.H., Hsu, J.L., Liu, G.H., Lee, S.H., Chen, N.H., Fang, J.T., 2022. Association of sleep, neuropsychological performance, and gray matter volume with glymphatic function in community-dwelling older adults. Neurology 98, E829–E838.
Sun, B.L., Wang, L.H., Yang, T., Sun, J.Y., Mao, L.L., Yang, M.F., Yang, X.Y., 2018. Lymphatic drainage system of the brain: a novel target for intervention of neurological diseases. Prog. Neurobiol. 163, 118–143.
Sun, X., Dias, L., Peng, C., Zhang, Z., Ge, H., Wang, Z., Chen, J.F., 2024a. 40 Hz light flickering facilitates the glymphatic flow via adenosine signaling in mice. Cell Discov 10, 81.
Sun, X.T., Dias, L., Peng, C.L., Zhang, Z.Y., Ge, H. T., Wang, Z.J., Chen, J.F., 2024. 40 Hz light flickering facilitates the glymphatic flow via adenosine signaling in mice. Cell Discovery, 10.
Tang, Y., Pasternak, O., Kubicki, M., Rathi, Y., Zhang, T., Wang, J., Seidman, L.J., 2019. Altered cellular white matter but not extracellular free water on diffusion MRI in individuals at clinical high risk for psychosis. Am. J. Psychiatry 176, 820–828.
Taoka, T., Masutani, Y., Kawai, H., Nakane, T., Matsuoka, K., Yasuno, F., Naganawa, S., 2017. Evaluation of glymphatic system activity with the diffusion MR technique: diffusion tensor image analysis along the perivascular space (DTI-ALPS) in Alzheimer's disease cases. Jpn. J. Radiol. 35, 172–178.
Terman, M., Terman, J.S., 2005. Light therapy for seasonal and nonseasonal depression: efficacy, protocol, safety, and side effects. CNS Spectr. 10, 647.
Thalén, B.E., Kjellman, B.F., Mørkrid, L., Wetterberg, L., 1995. Melatonin in light treatment of patients with seasonal and nonseasonal depression. Acta Psychiatr. Scand. 92, 274–284.
Tu, Y., Fang, Y., Li, G., Xiong, F., Gao, F., 2024. Glymphatic system dysfunction underlying schizophrenia is associated with cognitive impairment. Schizophr. Bull. 50, 1223–1231.
Ueda, R., Yamagata, B., Niida, R., Hirano, J., Niida, A., Yamamoto, Y., Mimura, M., 2024. Glymphatic system dysfunction in mood disorders: evaluation by diffusion magnetic resonance imaging. Neuroscience 555, 69–75.
van Veluw, S.J., Hou, S.S., Calvo-Rodriguez, M., Arbel-Ornath, M., Snyder, A.C., Frosch, M.P., Bacskai, B.J., 2020. Vasomotion as a driving force for paravascular clearance in the awake mouse brain. Neuron 105, 549–561.e545.
von Holstein-Rathlou, S., Petersen, N.C., Nedergaard, M., 2018. Voluntary running enhances glymphatic influx in awake behaving, young mice. Neurosci. Lett. 662, 253–258.
Williams, S.D., Setzer, B., Fultz, N.E., Valdiviezo, Z., Tacugue, N., Diamandis, Z., Lewis, L.D., 2023a. Neural activity induced by sensory stimulation can drive large-scale cerebrospinal fluid flow during wakefulness in humans. PLoS Biol. 21, e3002035.
Williams, S.D., Setzer, B., Fultz, N.E., Valdiviezo, Z., Tacugue, N., Diamandis, Z., Lewis, L.D., 2023b. Neural activity induced by sensory stimulation can drive large-scale cerebrospinal fluid flow during wakefulness in humans. PLoS Biol. 21.
Wirz-Justice, A., Bader, A., Frisch, U., Stieglitz, R.D., Alder, J., Bitzer, J., Riecher-Rössler, A., 2011. A randomized, double-blind, placebo-controlled study of light therapy for antepartum depression. J. Clin. Psychiatry 72, 986–993.
Wu, W., Zhao, Y., Cheng, X., Xie, X., Zeng, Y., Tao, Q., Lin, W.J., 2025. Modulation of glymphatic system by visual circuit activation alleviates memory impairment and apathy in a mouse model of Alzheimer's disease. Nat. Commun. 16, 63.
Xia, M.S., Yang, L., Sun, G.F., Qi, S., Li, B.M., 2017. Mechanism of depression as a risk factor in the development of Alzheimer's disease: the function of AQP4 and the glymphatic system. Psychopharmacology 234, 365–379.
Xie, L.L., Kang, H.Y., Xu, Q.W., Chen, M.J., Liao, Y.H., Thiyagarajan, M., Nedergaard, M., 2013. Sleep drives metabolite clearance from the adult brain. Science 342, 373–377.
Xiong, Y., Yu, Q.Y., Zhi, H.M., Peng, H.Y., Xie, M.J., Li, R.J., Sun, P., 2024. Advances in the study of the glymphatic system and aging. CNS Neurosci. Ther. 30.
Yan, C.G., Wang, X.D., Zuo, X.N., Zang, Y.F., 2016. DPABI: data processing & analysis for (resting-state) brain imaging. Neuroinformatics 14, 339–351.
Yao, D., Li, R., Hao, J.H., Huang, H.Q., Wang, X.B., Ran, L.S., Wang, M.H., 2023. Melatonin alleviates depression-like behaviors and cognitive dysfunction in mice by regulating the circadian rhythm of AQP4 polarization. Transl. Psychiatry 13.
Zang, Y., Jiang, T., Lu, Y., He, Y., Tian, L., 2004. Regional homogeneity approach to fMRI data analysis. Neuroimage 22, 394–400.
Zhang, D.J., Li, X.Y., Li, B.M., 2022a. Glymphatic system dysfunction in central nervous system diseases and mood disorders. Front. Aging Neurosci. 14.
Zhang, S., Zhang, Y., Ma, W.H., Qi, Z.Z., Wang, Y., Tao, Q., 2022b. Neural correlates of negative emotion processing in subthreshold depression. Soc. Cogn. Affect. Neurosci. 17, 655–661.
Zhang, W., Zhou, Y., Wang, J., Gong, X., Chen, Z., Zhang, X., Lou, M., 2021. Glymphatic clearance function in patients with cerebral small vessel disease. Neuroimage 238, 118257.
Zhao, D., Wang, J., Zhu, Y., Zhang, H., Ni, C., Zhao, Z., Tong, Z., 2025. Targeting the glymphatic system: Aβ accumulation and phototherapy strategies across different stages of Alzheimer's disease. Transl. Neurodegener. 14, 49.
Zou, K.L., Deng, Q.W., Zhang, H., Huang, C.S., 2024. Glymphatic system: a gateway for neuroinflammation. Neural Regen. Res. 19, 2661–2672.